Title

FREQUENCY SELECTIVE NMR FULSE SEQUENCES GENERATED BY ITERATIVE SCHEMES WITH MULTIPLE FIXED POINTS

Authors

Cho, H.
Mueller, K.T.
Shaka, A.J.

Publication Date

1988-09-01

LBL-25943
Preprint

Lawrence Berkeley Laboratory
UNIVERSITY OF CALIFORNIA

Materials & Chemical Sciences Division

Submitted to Chemical Physics

Frequency Selective NMR Pulse Sequences Generated by Iterative Schemes with Multiple Fixed Points

H. Cho, K.T. Mueller, A.J. Shaka, and A. Pines

September 1988

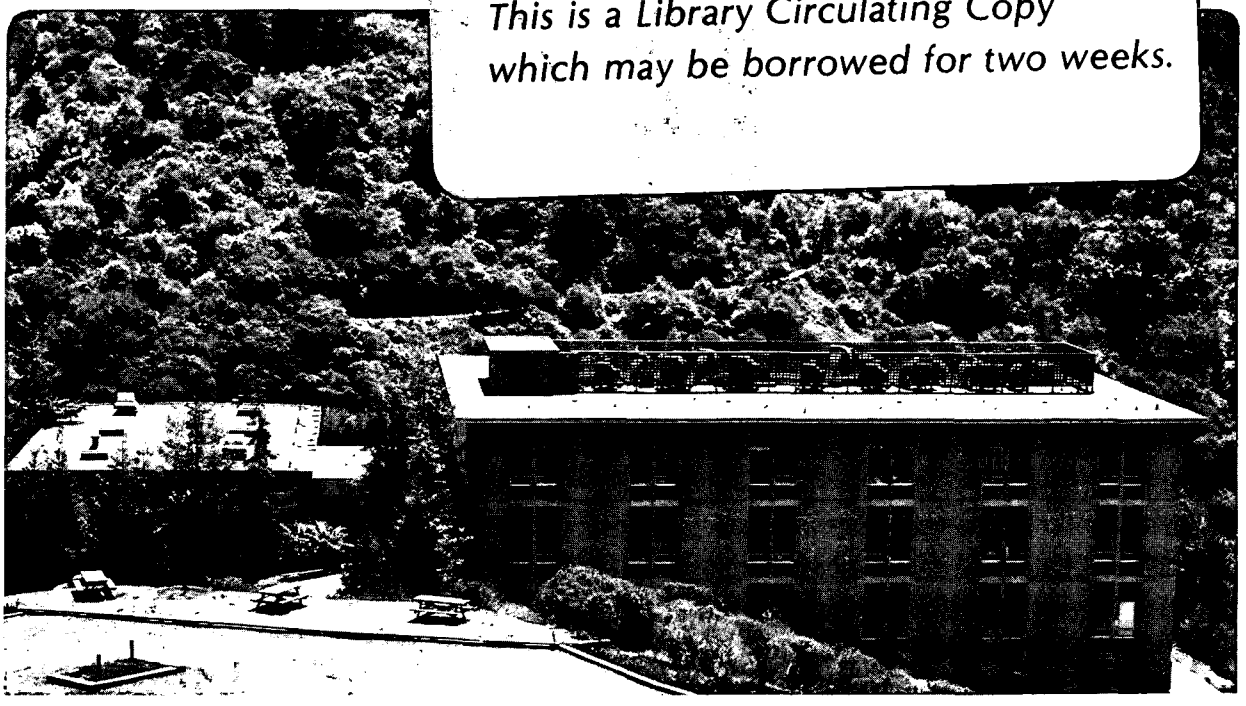

Prepared for the U.S. Department of Energy under Contract Number DE-AC03-76SF00098.

DISCLAIMER

LBL-25943

FREQUENCY SELECTIVE NMR PULSE SEQUENCES GENERATED BY ITERATIVE SCHEMES WITH MULTIPLE FIXED POINTS

H. Cho†, K. T. Mueller, A. J. Shaka††, and A. Pines

Materials and Chemicals Sciences Division
Lawrence Berkeley Laboratory
1 Cyclotron Road
Berkeley, California 94720

and

Department of Chemistry
University of California
Berkeley, California 94720

†Present address: Laboratorium für Physikalische Chemie,
ETH-Zentrum, CH-8092 Zürich, Switzerland

††Present address: Department of Chemistry, University of California,
Irvine, California 92717

Running title: Frequency Selective NMR Pulse Sequences ...

ABSTRACT

General methods drawn from the subject of nonlinear dynamics and iterative mappings are employed to demonstrate how selective excitation sequences for nuclear magnetic resonance experiments may be developed. The relevance of iterative maps with more than one fixed set to iterative schemes for frequency selective excitation is examined. Specific sequences are proposed for selective inversion of spins depending on their shifts from the frequency of the incident radiofrequency field.

I. INTRODUCTION

The use of modulated, coherent pulses to compensate for insufficient irradiation power and other common deficiencies of the radiation source is a technique of well-documented utility and effectiveness in nuclear magnetic resonance (NMR) and optical spectroscopy. The first examples of these "composite pulses" inverted the populations of the nuclear spin Zeeman energy levels in weakly coupled spin systems over broad ranges of transition frequencies.[1] This operation is known in NMR terminology as a π rotation, or population inversion. It can be accomplished with a single pulse, but only over a narrow range of resonance frequencies limited by the amount of radiofrequency (rf) power available.

Since the advent of composite pulses, several workers have described composite pulses which, in contrast to the broadband sequences, invert spin populations over narrow and tailored bandwidths.[2-9] Sequences with these features are essential components of NMR experiments requiring that nuclear spins be preferentially excited according to the value of some selected parameter. Examples of these kinds of experiments include selective heteronuclear decoupling in liquids,[10] solvent suppression in high resolution NMR,[11] selective spin locking,[12] chemical exchange studies,[13] NMR imaging,[14] topical NMR,[15] heteronuclear zero-field NMR,[16] nk-quantum selective NMR,[17] and 3-D NMR.[18]

For a pulse sequence to invert one group of spins and not some other

group lying in an rf field ω_1 differing from that of the first group by an amount $\delta\omega_1$, it is evident that the irradiation period must equal or exceed $\pi/\delta\omega_1$.[19] For finer selectivity the length of the sequence must increase accordingly. The importance of long pulsed excitation sequences for pulsed NMR has motivated the development of several theoretical formalisms for designing and analyzing these sequences. One of the most recent is an approach by Warren et al.,[20] based on the use of iterative schemes to generate pulse sequences. In many cases, sequences are known which can approximately excite the desired response. A single π pulse, for instance, approximates a selective inversion sequence. Instead of developing pulse sequences from scratch, in an iterative scheme approach pulse sequences are derived by performing a repetitive algorithm, starting with the approximate sequence as the first iterate. The theoretical task, then, is to determine the algorithm which, when applied to the initial sequence S_0, generates higher iterate sequences with successively improved properties. A general theoretical treatment of this method has been given by Tycko, et al.[3,6]

Recently, a family of sequences has been developed by this technique that can excite a true, tailored inversion of spin populations in a NMR experiment.[6,7] On resonance, these bandpass sequences selectively and completely invert nuclear spin populations depending on the rf strength at the spin position. Moreover, spins lying outside the inversion passbands are left unperturbed from their original equilibrium position. Two

families of iterative schemes are introduced in this paper for generating analogous composite π pulses capable of selectively inverting nuclear spin poulations over sharply defined ranges of *resonance frequencies.* Unlike previously reported sequences,[12] the sequences introduced here are windowless, contain only constant amplitude, variable phase pulses, and bring about complete inversion of spin populations over their passbands. Both theoretical and experimental evidence are presented, and an application of one of these sequences to selective signal inversion in liquid state NMR is briefly discussed.

II. THEORY

A general theory of iterative schemes and its application to specific problems in NMR have been reported in several prior publications by Tycko, et al.[3,6] In the language of this formalism, iterative schemes can be represented mathematically as a transformation of the nuclear spin propagator. If we write the propagator for some initial pulse sequence as U_0, then the nuclear spin propagator corresponding to the sequence obtained by operating once with an iterative scheme can be written:

$$U_1 = F(U_0) \qquad (1)$$

where F is a mapping on the propagator space. The form of F is determined by the operations performed on the pulse sequence to generate the next

iterate, while the mathematical form of the propagators depends on both the particular iterative scheme and the experimental parameters of the radiofrequency field and the spin system.

The iterative schemes we consider here can be denoted by a list of phase shifts, $[\phi_1, \phi_2, \ldots, \phi_N]$. Each successive iterate is constructed by phase shifting an input pulse sequence about the z-axis N times using the phase shifts in the list, and then concatenating the N phase shifted versions of the input sequence. The bandwidth properties of the sequences generated by iterative schemes are specified by the stability of the fixed points of the mapping F. Iterative schemes corresponding to maps with more than one fixed set, for example, can lead to sequences which perform bandpass excitation.

The objective is to find an iterative scheme having a map F with the property that for some values of the rf carrier frequency ω_0 the iterates of the function approach one stable fixed set, while for other values $\omega_0 \pm \Delta\omega$ the series of iterates approaches a second value. One way this objective can be realized is to precede an iterative function F, with known stability properties, by a prior sequence, or premapping. This may lead to a scheme with chaotic properties, but by choosing an S_0 which is close to the desired profile it is possible to obtain good results for low numbers of iterations. A second new family of schemes is generated by strictly forcing the mapping to be unconditionally stable, and involves using

inverses in the iteration process to generate a mapping with two regions of stability.

A useful premapping is shown schematically in figure 1 as a function of the propagator space SO(3). For the simplest system, that of uncoupled spin-1/2 nuclei, all possible propagators assume the form of quantum mechanical rotation operators, and thus are contained in this three dimensional space of rotations.[23] This particular function, described by the iterative scheme [0,180,90,270,270,90,180,0] has a complex flow of points globally, but within certain regions of SO(3) the trajectories of points generated by this scheme can be deduced a priori. All points in the xy plane of SO(3), for instance, are mapped after a single iteration to the origin. Therefore, rotations about axes in the xy plane become the identity operation.

A second region of interest are the points in the neighborhood of rotations of the form $R(\alpha_0)$ where:

$$\alpha_0 = 2\pi/(3\sqrt{3})\ [\sqrt{2}\cos\varphi\ ,\sqrt{2}\sin\varphi\ ,\pm 1] \qquad (2)$$

These vectors define points in SO(3) representing 120^o rotations about axes separated from the plus and minus z-axis by the magic angle. Points in SO(3) of this form are mapped after one iteration to $R(\alpha_1)$, where:

$$\alpha_1 = \pi\,[\cos\varphi\,,\ \sin\varphi\,,\ 0] \qquad (3)$$

Rotations of this type lie on the equator of SO(3), and are therefore inversion operations.

Points in the neighborhood of the operators defined by $R(\alpha_0)$ lie approximately above and below the set of operators $R_\psi(\pi/2)$ in SO(3) which correspond to 90 degree rotations.[3] The set of rotation operators corresponding to single, off-resonance pulses lie within this region for some set of resonance offset values. These points will therefore be mapped close to the equator by the iterative function corresponding to [0,180,90,270,270,90,180,0]. So single, off-resonance $\pi/2$ pulses are approximately converted to π pulses by this mapping, while single, on-resonance pulses are converted by this scheme into cycles. At this stage, the points mapped to the neighborhood of the equator can be mapped even closer by applying a second mapping with the equator as a stable fixed set. It is also necessary that the origin be a stable fixed point of the second iterative sequence, and this can be accomplished with a scheme such as [0,330,60,330,0].[3]

A second family of selective resonance offset pulse sequences can be found by examination of the theoretical development of a set of rf amplitude selective iterative schemes reported earlier.[6] Two schemes were found which had the equator and origin of SO(3) as stable fixed

points. The symmetry properties of these schemes necessitates the existence of an unstable fixed set in between, located in the xy plane of SO(3). Points on either side, corresponding to different values of the rf amplitude of the pulses, are mapped to one or the other of the fixed sets resulting in bandpass behavior. The usefulness of these schemes is therefore largely restricted to spin propogators described by rotations lying in the xy plane of SO(3).

In the process of determining these schemes, the stability of the fixed sets is assessed by making a linear approximation of the three dimensional mapping in the neighborhood of the fixed sets, and solving for the eigenvalues of the linearized mapping. For these mappings, the z direction is an eigenvector with the eigenvalue N, where N is the number of phase shifts in the iterative scheme. This produces the inherent instability along the z-axis since the eigenvalue is greater than unity. However, if one includes inverses in the iterative scheme, the eigenvalue may be different from N. The inverse of a rotation $R(\alpha_j)$ is a theoretical construct defined by the relation:[5,21,22]

$$R(\alpha_j)\,(R(\alpha_j))^{-1} = 1 \qquad (4)$$

The inverse of the rotation operation produced by a single pulse is obtained by adding 180^{o} to the phase of the pulse and reversing the sign of the offset. Experimental realization of inverse sequences is discussed elsewhere.[22] In the case that the number of regular shifts and inverse

shifts in a sequence differ by one, the z eigenvalue is unity and the scheme may have stability in the z direction leading to possible bandpass inversion behavior as a function of resonance offset.

The scheme [0,15,180,165,270,165,180,15,0] has been shown to produce bandpass behavior as a function of rf amplitude[6]. We now introduce the scheme:

$$[0,(195)^{-1},180,(345)^{-1},270,(345)^{-1},180,(195)^{-1},0]$$

where $(..)^{-1}$ denotes an inverse, which has the property of bandpass selectivity as a function of *both* ω_1 and $\Delta\omega$. The same behavior is expected on-resonance for the new sequence since all of the inverse pulses are simply shifted by 180^{o} about the z-axis, while the flow of points in SO(3) is now stable along the z-axis leading to resonance offset bandpass inversion. In fact, every point on the z-axis can be shown to be a stable fixed point, which are attractors and determine the behavior of a set of points in SO(3). Points on the z-axis correspond to a trivial phase shift of the magnetization about the z-axis and therefore do not affect the z component of the magnetization.

III. RESULTS AND DISCUSSION

The outcome of following the premapping with an iterative scheme

which generates broadband π pulses appears in figure 2. This figure shows computer simulations and experimental results of the population inversion as a function of the shift of the rf frequency from the spin resonance frequency for several pulse sequences. Experimental data for two sequences are displayed, one an eight pulse sequence produced by iterating once with the scheme [0,180,90,270,270,90,180,0] on a single pulse, and the other a forty pulse sequence produced by operating upon the previous eight pulse sequence with the scheme [0,330,60,330,0]. The two sequences produced by the iterative procedure are written out explicitly in Table I.

These data confirm that for some values of ω_0 higher and lower than the actual spin resonance frequency, the premapping transforms the off-resonance propagator to an operator approximately of the form $R_{\psi'}(\pi)$. Following the premapping with the broadband π scheme maps these rotation operators even closer to the equator of SO(3). On-resonance $\pi/2$ pulses become cyclic sequences by this iteration scheme. Near resonance for these sequences, therefore, the spins remain in their equilibrium states and no inversion takes place.

A computer drawn basin image[3,6] for this scheme appears in figure 3. The premapping step has been counted as the first iteration. This image was computed by checking the convergence of points in SO(3) to the equator upon iteration, and this is a slice of SO(3) containing the z-axis.

Convergence was decided when a point was mapped to within $\pm 5^{o}$ of the equator. As anticipated, large regions above and below the transverse plane converge to the equator. A narrow region encompassing the xy plane where the basin is discontinuous and chaotic lies between the two main basins of the equator. The discontinuities in this transition region are revealed in the third inversion plot of figure 2 by the sharp oscillations between the range of ω_0 values where there is complete inversion, and the region where there is no inversion.

Two features of the basin image deserve mention. First is the twofold reflection symmetry. The reflection symmetry about the plane containing the z-axis is a consequence of the z rotational symmetry of phase shift schemes.[3] The reflection symmetry through the xy plane comes about because of the phase symmetry of the two iterative schemes defining the mapping.[3]

Secondly, it should be noted that unlike schemes presented earlier,[3,6] the stable fixed set of this premapped function, viz., the equator, is not situated in the middle of its basin. The premapping function defined by the scheme [0,180,90,270,270,90,180,0] does not have the equator as a fixed set. The points in SO(3) mapped to the equator are indicated by the large, light regions above and below the xy plane of SO(3).

The theoretical results from iterating a single π pulse with the mapping $[0,(195)^{-1},180,(345)^{-1},270,(345)^{-1},180,(195)^{-1},0]$ are shown

in figures 4 and 5. The nine and eighty-one pulse sequences are written out explicitly in Table II.

These figures clearly show that including inverse pulses produces sharp bandpass behavior with full inversion within a well-defined region of resonance offsets and no inversion outside of this region. As one iterates to longer pulse sequences, the cutoff becomes sharper as shown in figure 4 where the inversion profiles for the nine, eighty-one, and seven-hundred-twenty-nine pulse sequences are presented as a function of normalized resonance offset. The behavior as a function of both resonance offset and rf amplitude is shown in the contour plot of figure 5 for the eighty-one pulse sequence. The contours represent the values of $\Delta\omega$ and ω_1 where the inversion reaches values of 0.99, 0.0, and -0.99. Within the 0.99 region, all of the magnetization is essentially fully inverted, while outside of the -0.99 contour, there is no net disturbance of the magnetization.

The basin map for this scheme, shown in figure 6, has been computed with two convergence criteria; either a mapping to within $\pm 5^{o}$ of the equator or to within $\pm 5^{o}$ of the z-axis. When computed with each exclusive criterion, it is determined that the inner region about the origin does indeed map only to the z-axis, while the outer region is the basin of the equator. The unstable fixed set is visible as the dark band between these regions. Therefore, one expects that for some values of the resonance offset, and not others, the spins are inverted by pulse

sequences created by the iterative schemes which are represented by this mapping.

Figure 7 indicates that the bistable forty pulse sequence derived with the premapping may be employed to selectively invert nuclear spins depending on their chemical shift. Three spectra obtained with this sequence graphically depict some manifestations of a selective inversion experiment. Two proton resonances, one corresponding to liquid benzene, the other acetone, are present in the conventional NMR spectrum at the top. The bottom spectrum was obtained by selectively inverting the acetone protons with the forty pulse sequence immediately prior to recording the free induction decay (FID). The middle spectrum demonstrates the suppression of the acetone peak by selective inversion. The suppression of this peak was accomplished by selective inversion of the acetone resonance followed by a period during which the acetone peaks are allowed to relax. If a $\pi/2$ pulse is given at the null point, i.e., the time at which the acetone spins have relaxed to saturation, and the FID measured, the spectrum in the middle of figure 7 results. In such a manner, suppression of chosen peaks in a multiline NMR spectrum is possible.

IV. EXPERIMENTAL

All experiments were performed on a homebuilt spectrometer in an

8.4 T magnetic field. Distilled water was used for the measurements of figure 2, while the selective inversion experiments of figure 7 were performed on a mixture of approximately equal volumes of acetone and benzene. Both samples were sealed in 1.5 mm capillary tubes.

The sequences requiring pulses with phases other than the four standard quadrature phases were generated by routing the rf through two tunable rf quadrature circuits connected in series. Two channels of the second circuit were adjusted to produce switched rf outputs with a relative phase of 60^{o}. All necessary phase shifts could be produced by appropriate combinations of the phases of the two circuits.

The input to the phase shifting apparatus was a variable frequency rf synthesizer, while the rf for the receiver section and read pulses was generated by a fixed, on-resonance rf source. This arrangement allowed on-resonance detection to be performed while employing variable off-resonance excitation. The relative phases and amplitudes of all of the pulses were set using a vector voltmeter, and the $\pi/2$ times were calibrated by standard techniques.

The inversion performance of the pulse sequences was determined by following each sequence with an on-resonance $\pi/2$ read pulse after a dephasing delay of 150 ms. The rf amplitudes of the eight pulse and the forty pulse sequences were 10.82 and 11.36 kHz, respectively, while the read pulses were 109 khz. The free induction decay aquired after each

read pulse was Fourier-transformed, and the height of the absorption signal was measured and normalized to assess the degree of population inversion.

The acetone/benzene spectra were obtained by setting the rf carrier to the resonance frequency of the benzene protons. The rf amplitude was calibrated to be 3.62 kHz, which, with the observed resonance offset difference of 1.95 kHz, corresponds to value for $\Delta\omega/\omega_1{}^0$ of 0.54. The spectrum with the inverted acetone peak was recorded by repeating the experiment as described above with the forty pulse sequence, while the selective saturation was performed by allowing the acetone spins to relax for 8.25 s. before applying the read pulse.

V. CONCLUSION

The unique and general insights to be found by viewing iterative schemes as mappings on a propagator space have been employed here to discover windowless, chemical shift selective inversion sequences. These methods suggest that premapping can be incorporated into an iterative scheme to derive pulse sequences with bandpass excitation selectivity. The selectivity of the sequence here is extremely sharp, as indicated by the fact that the interval between the frequencies where there is complete inversion and the regions where there is no inversion comes within a factor of three of the theoretical minimum imposed by the

length of the excitation period. The entire sequence is windowless and contains only readily calibrated $\pi/2$ and π pulses.

Another set of windowless sequences of π pulses was also introduced using inverse pulses. These schemes are bandpass selective in both resonance offset and rf amplitude, inverting spins completely within a well-defined range of both parameters.

The practical utility of techniques for frequency selective excitation are well-known, and have been mentioned earlier. The inversion and suppression of selected lines in an NMR spectrum are just two simple examples of the special properties of bandpass specific sequences.

ACKNOWLEDGEMENTS

KTM is a National Science Foundation Graduate Fellow. This work was supported by the Director, Office of Energy Research, Office of Basic Energy Sciences, Materials Sciences Division of the U.S. Department of Energy under Contract No. DE-AC03-76SF00098.

REFERENCES

1. M. H. Levitt and R. Freeman, J. Magn. Reson. **33** (1979) 473.
2. R. Tycko and A. Pines, Chem. Phys. Lett. **111** (1984) 462.
3. R. Tycko, A. Pines, and J. Guckenheimer, J. Chem. Phys. **83** (1985) 2775.
4. M. H. Levitt, Prog. Nucl. Magn. Reson. Spectrosc. **18** (1986) 61.
5. A. J. Shaka and R. Freeman, J. Magn. Reson. **59** (1984) 169.
6. H. Cho, J. Baum, and A. Pines, J. Chem. Phys. **86** (1987) 3089.
7. H. Cho, R. Tycko, A. Pines, and J. Guckenheimer, Phys. Rev. Lett. **56** (1986) 1905.
8. J. Baum, R. Tycko, and A. Pines, Phys. Rev. A**32** (1985) 3435.
9. M. S. Silver, R. I. Joseph, and D. I. Hoult, J. Magn. Reson. **59** (1984) 347.
10. L. Mueller, A. Kumar, and R. R. Ernst, J. Chem. Phys. **63** (1975) 5490.
11. A. G. Redfield, S. D. Kunz, and E. K. Ralph, J. Magn. Reson. **19** (1975) 114.
12. G. A. Morris and R. Freeman, J. Magn. Reson. **29** (1978) 433.
13. F. W. Dahlquist, K. J. Longmuir, and R. B. DuVernet, J. Magn. Reson. **17**, (1975) 406.
14. P. G. Morris, Nuclear Magnetic Resonance Imaging in Medicine and Biology (Clarendon, Oxford, 1986).
15. J. J. H. Ackerman, T. H. Grove, G. G. Wong, D. G. Gadien, and G. K. Redda, Nature **283** (1980) 167; C. Segebarth, P. R. Luyten, and J. A. denHollander, J. Magn. Reson. **75** (1987) 345, and references therein.

16. D. B. Zax, A. Bielecki, K. W. Zilm, A. Pines, and D. P. Weitekamp, J. Chem. Phys. **83** (1985) 4877.

17. W. S. Warren, S. Sinton, D. P. Weitekamp, and A. Pines, Phys. Rev. Lett. **43** (1979) 1791.

18. C. Griesinger, O. W. Sorenson, and R. R. Ernst, J. Am. Chem. Soc. **109** (1987) 7227.

19. H. M. Cho, Ph.D. dissertation, University of California, Berkeley, 1987, published as Lawrence Berkeley Laboratory Report No. LBL-22993.

20. W. S. Warren, D. P. Weitekamp, and A. Pines, J. Chem. Phys. **73** (1980) 2084.

21. A. J. Shaka, J. Keeler, and R. Freeman, J. Magn. Reson. **53** (1983) 313.

22. M. H. Levitt and R. R. Ernst, J. Magn. Reson. **55** (1983) 247.

23. H. Goldstein, Classical Mechanics, 2nd ed. (Addison-Wesley, Reading, 1977).

TABLES

Table I: Two pulse sequences generated by the iterative procedure which includes a premapping as described in the text. Both sequences consist of a series of fixed amplitude $\pi/2$ pulses with no spacing between the pulses. The numbers below designate the phase, in degrees, to be associated with each of the pulses in the sequence. The lengths of the two sequences are eight $\pi/2$ pulses for the first, and forty $\pi/2$ pulses for the second.

A. 0, 180, 90, 270, 270, 90, 180, 0

B. 0, 180, 90, 270, 270, 90, 180, 0,
330, 150, 60, 240, 240, 60, 150, 330,
60, 240, 150, 330, 330, 150, 240, 60,
330, 150, 60, 240, 240, 60, 150, 330,
0, 180, 90, 270, 270, 90, 180, 0

Table II: Two pulse sequences generated by the iterative procedure employing inverse pulses. The sequences are of fixed amplitude π pulses and the numbers indicate the phase of each of the pulses, while $(...)^{-1}$ represents an inverse pulse as described in the text. The lengths of sequences C and D are nine and eighty-one pulses respectively.

C. $0, (195)^{-1}, 180, (345)^{-1}, 270, (345)^{-1}, 180, (195)^{-1}, 0$

D. $0, (195)^{-1}, 180, (345)^{-1}, 270, (345)^{-1}, 180, (195)^{-1}, 0$
$(195)^{-1}, 30, (15)^{-1}, 180, (105)^{-1}, 180, (15)^{-1}, 30, (195)^{-1},$
$180, (15)^{-1}, 0, (165)^{-1}, 90, (165)^{-1}, 0, (15)^{-1}, 180,$
$(345)^{-1}, 180, (165)^{-1}, 330, (255)^{-1}, 330, (165)^{-1}, 180, (345)^{-1},$
$270, (105)^{-1}, 90, (255)^{-1}, 180, (255)^{-1}, 90, (105)^{-1}, 270,$
$(345)^{-1}, 180, (165)^{-1}, 330, (255)^{-1}, 330, (165)^{-1}, 180, (345)^{-1},$
$180, (15)^{-1}, 0, (165)^{-1}, 90, (165)^{-1}, 0, (15)^{-1}, 180,$
$(195)^{-1}, 30, (15)^{-1}, 180, (105)^{-1}, 180, (15)^{-1}, 30, (195)^{-1},$
$0, (195)^{-1}, 180, (345)^{-1}, 270, (345)^{-1}, 180, (195)^{-1}, 0$

FIGURE CAPTIONS

Figure 1: Flow of selected regions in SO(3) for the map of the iterative scheme [0, 180, 90, 270, 270, 90, 180, 0]. All points on the transverse plane are mapped to the origin; all points in the neighborhood of the coordinates defined by equation (2), designated by points labelled 1, are mapped to the equator.

Figure 2: Inversion as a function of normalized resonance offset for (a) the eight pulse sequence in Table I, (b) the forty pulse sequence in Table I, and (c) the two hundred pulse sequence generated by iterating once on the forty pulse sequence with the scheme [0, 330, 60, 330, 0]. All pulses are of length $\pi/2$ when calibrated on-resonance. Experimental data are shown as black dots in (a) and (b). The discontinuities in the basin image (see figure 3) near the xy plane are manifested by the chaotic variations in the inversion in (c) between the region where there is no inversion, and the regions where there is complete inversion.

Figure 3: Two dimensional basin image through a slice of SO(3) containing the z-axis of the map specified by the scheme [0, 330, 60,330, 0], preceded by the premapping step [0, 180, 90, 270, 270, 90, 180, 0]. The basin shown is of the equator, and can be identified by the light colored regions within the circle. The gray scale to the left assigns the correspondence between the shade at a point and the number of iterations necessary to map the point to the equator.

Figure 4: Plots of inversion as a function of resonance offset for (0) a single π pulse, (1) the nine pulse sequence of Table II, (2) the eighty-one pulse sequence of Table II, and (3) the seven hundred and twenty-nine pulse sequence obtained by one further iteration. Here, all pulses are π pulses if given on-resonance. The whole of SO(3) lies within the basin of one or the other of the two fixed sets excluding the unstable boundary in between, and the inversion profiles therefore become more strictly bandpass as the number of iterations increases.

Figure 5: Contour plots of inversion profiles as a function of both resonance offset and rf amplitude for (a) a single π pulse, (b) the nine pulse sequence of Table II, (c) the eighty-one pulse sequence of Table II, and (d) the seven hundred and twenty-nine pulse sequence obtained by one further iteration. The contours shown are those where extent of the inversion is 0.99, 0, and -0.99. The bandpass behavior is evident as a function of both parameters, and improves in all directions as the number of iterations increases.

Figure 6: Two dimensional basin map of a slice of SO(3) containing the z-axis for $[0,(195)^{-1},180,(345)^{-1}, 270(345)^{-1},180,(195)^{-1},0]$. The behavior of the flow is smooth, and the unstable fixed set between the two stable fixed sets (the z-axis and the equator) is visible as the dark band between the two lighter areas. The basins shown are that of the equator and the z-axis, both of which lie entirely within their basins.

Figure 7: NMR spectra of a liquid benzene/acetone solution. At the top is the conventional spectrum, while at the bottom is the spectrum obtained by inverting the acetone resonance before recording the FID. The middle spectrum is that obtained by selectively inverting the acetone resonance and allowing it to relax to saturation before recording the FID. The forty pulse sequence of Table I was used to accomplish the selective excitation. All spectra are plotted with the same absolute intensity scale, showing that there is little loss of intensity in the bottom two spectra as a result of the prior irradiation with the forty pulse sequence.

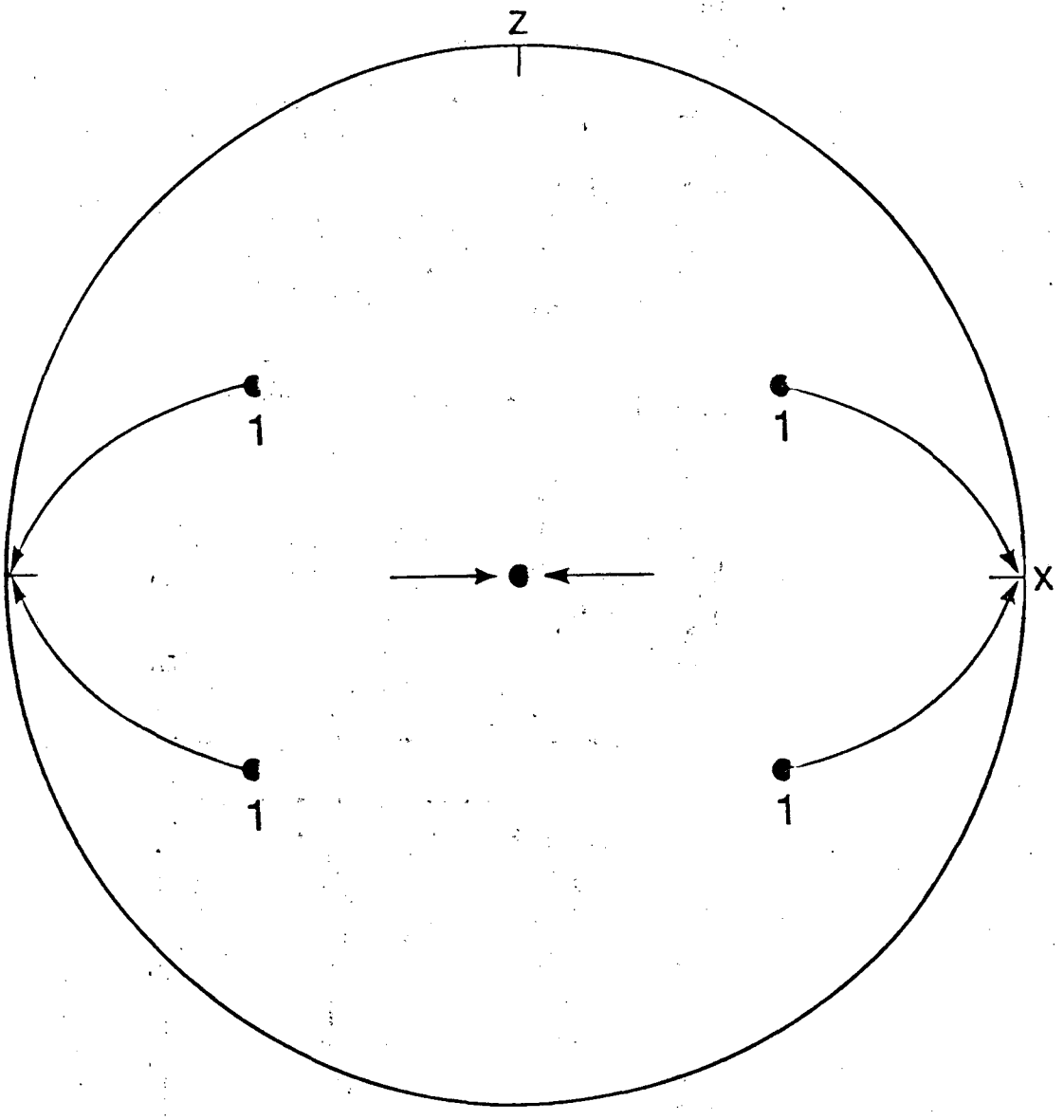

XBL 881-282

Figure 1

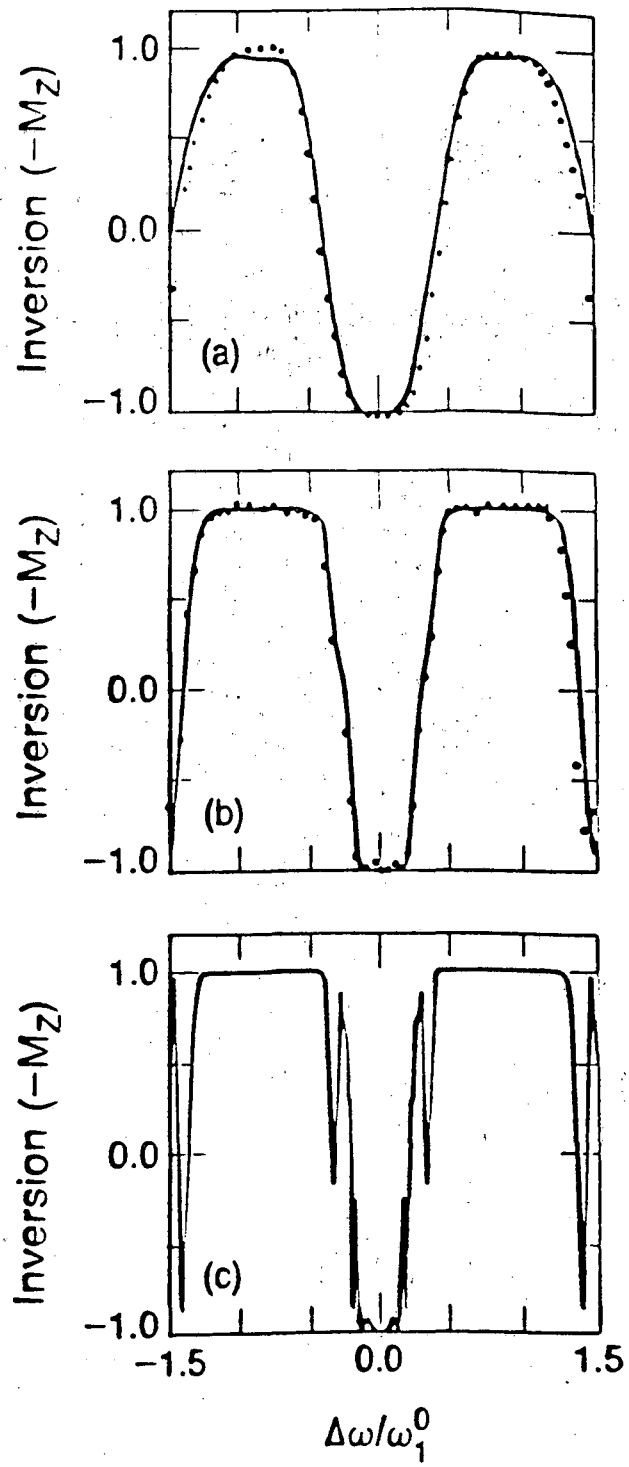

XBL 874 6277

Figure 2

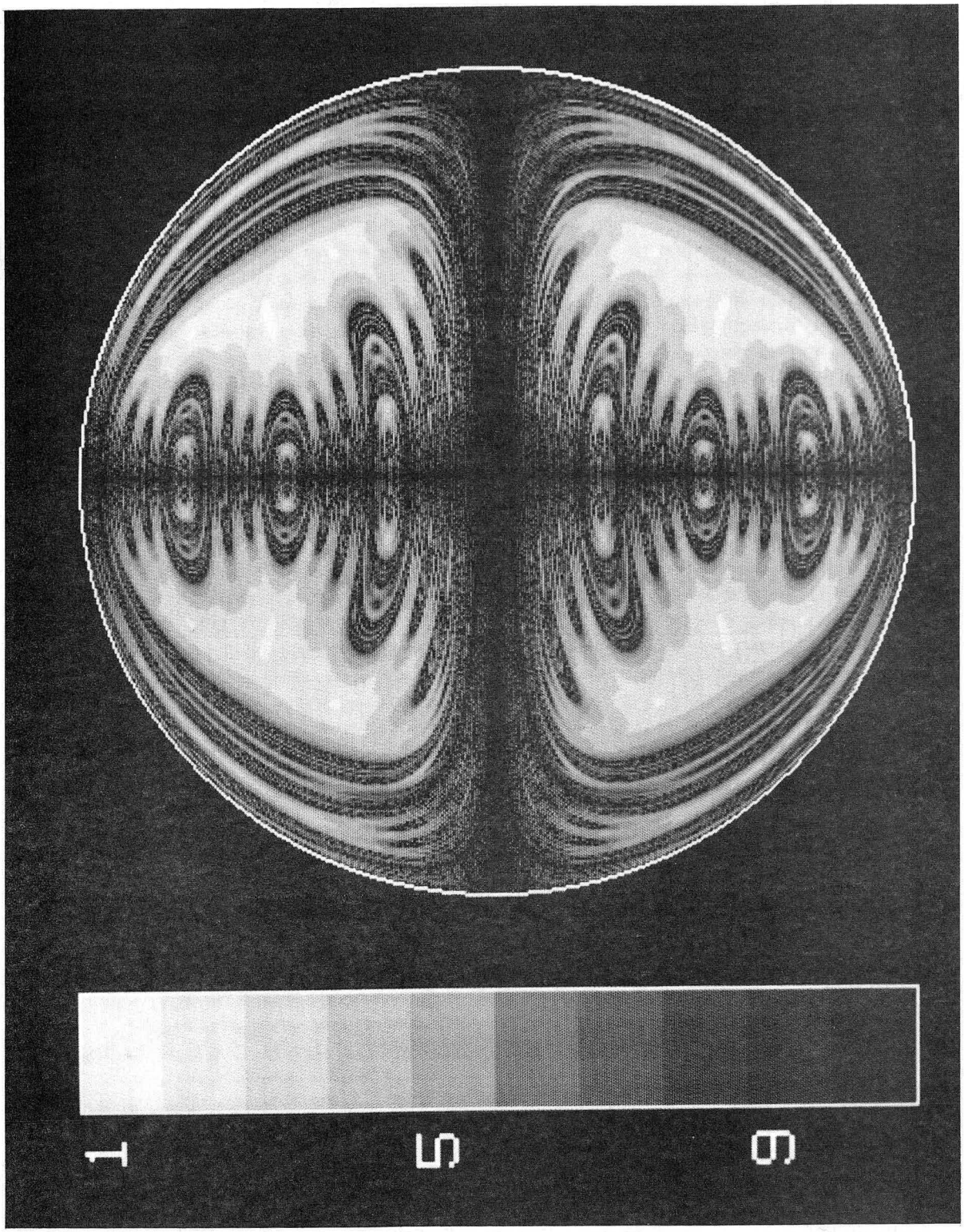

Figure 3

XBB 888-7859

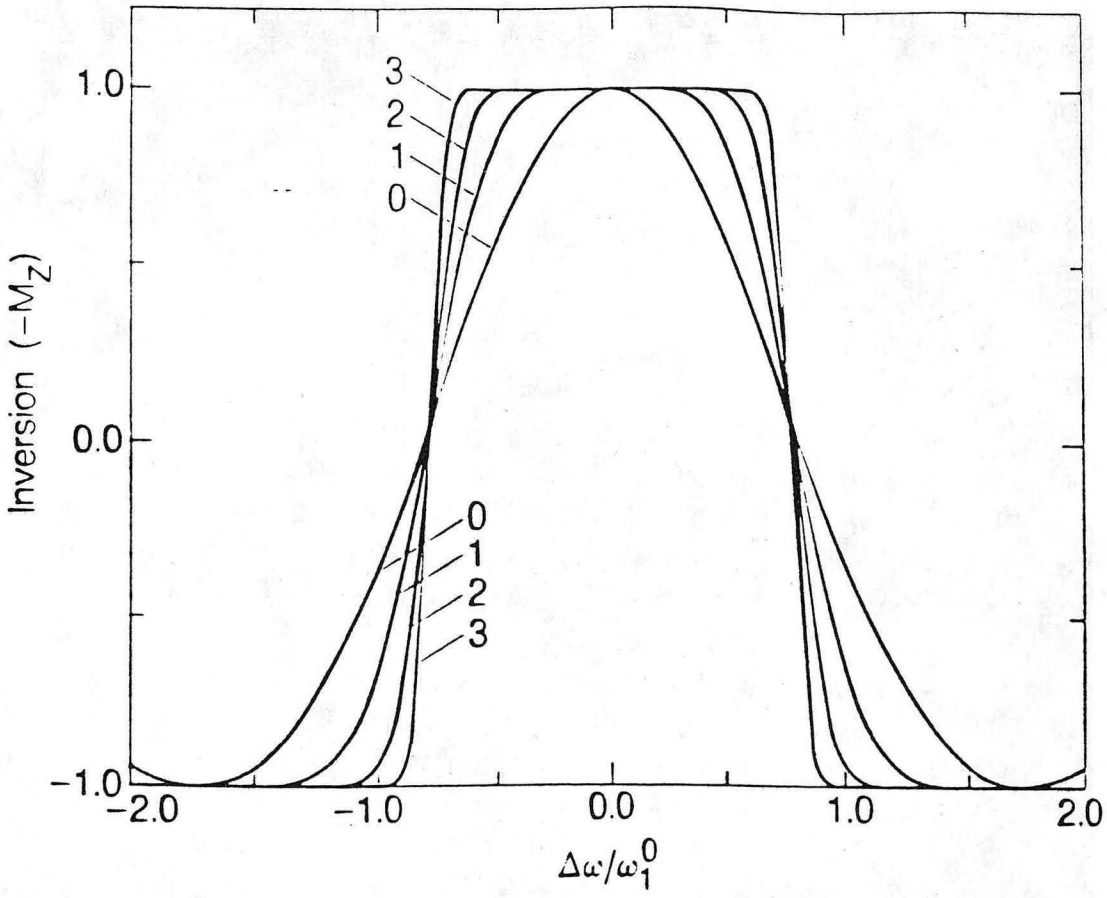
1.0
0.0
-1.0
Inversion (-M_Z)
-2.0
-1.0
0.0
1.0
2.0
$\Delta\omega/\omega_1^0$
3
2
1
0
0
1
2
3
XBL 888-8530

Figure 4

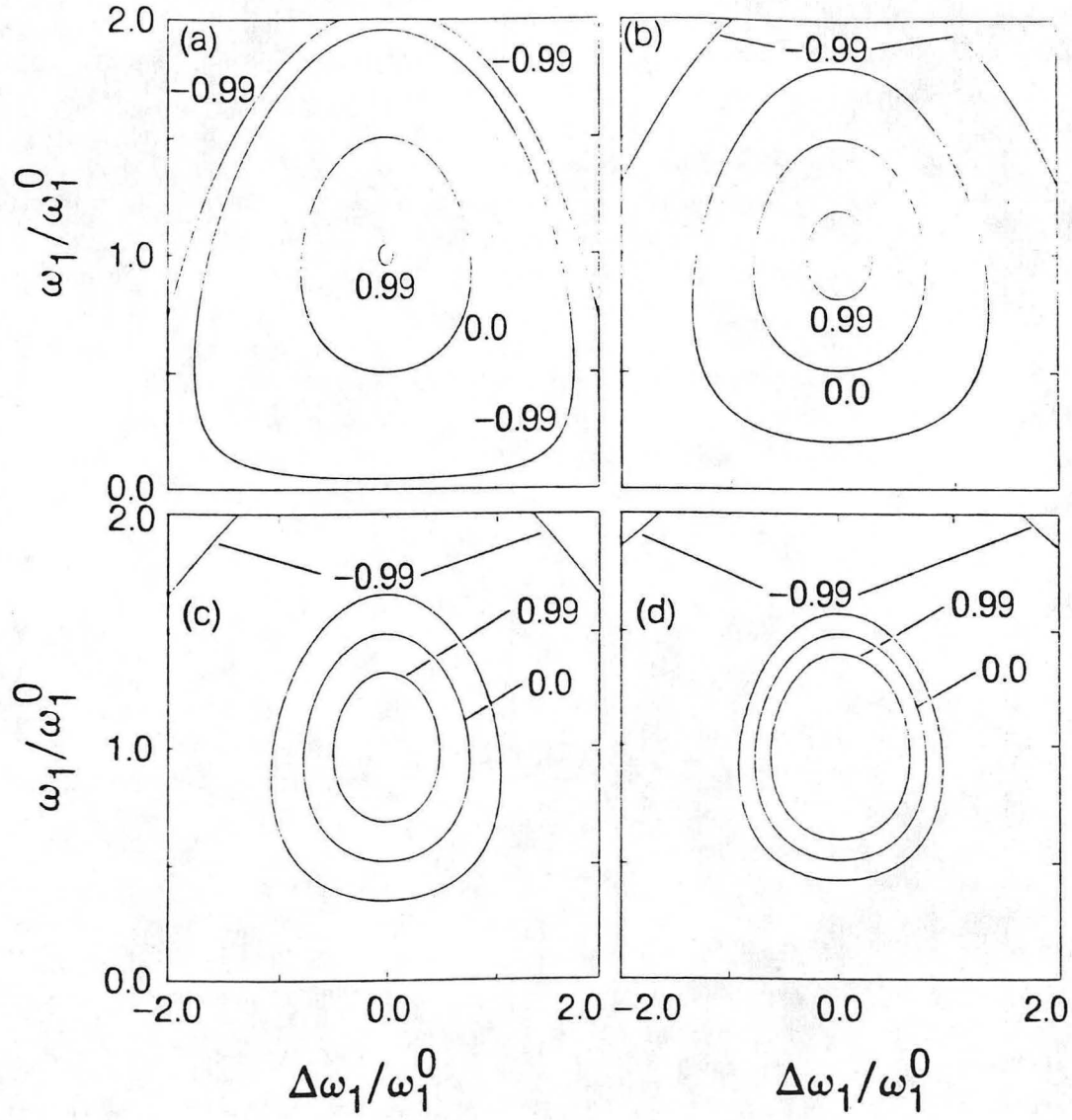
(a)
(b)
(c)
(d)
-0.99
0.99
0.0
2.0
1.0
0.0
-2.0
ω_1/ω_1^0
$\Delta\omega_1/\omega_1^0$
XBL 888-8531

Figure 5

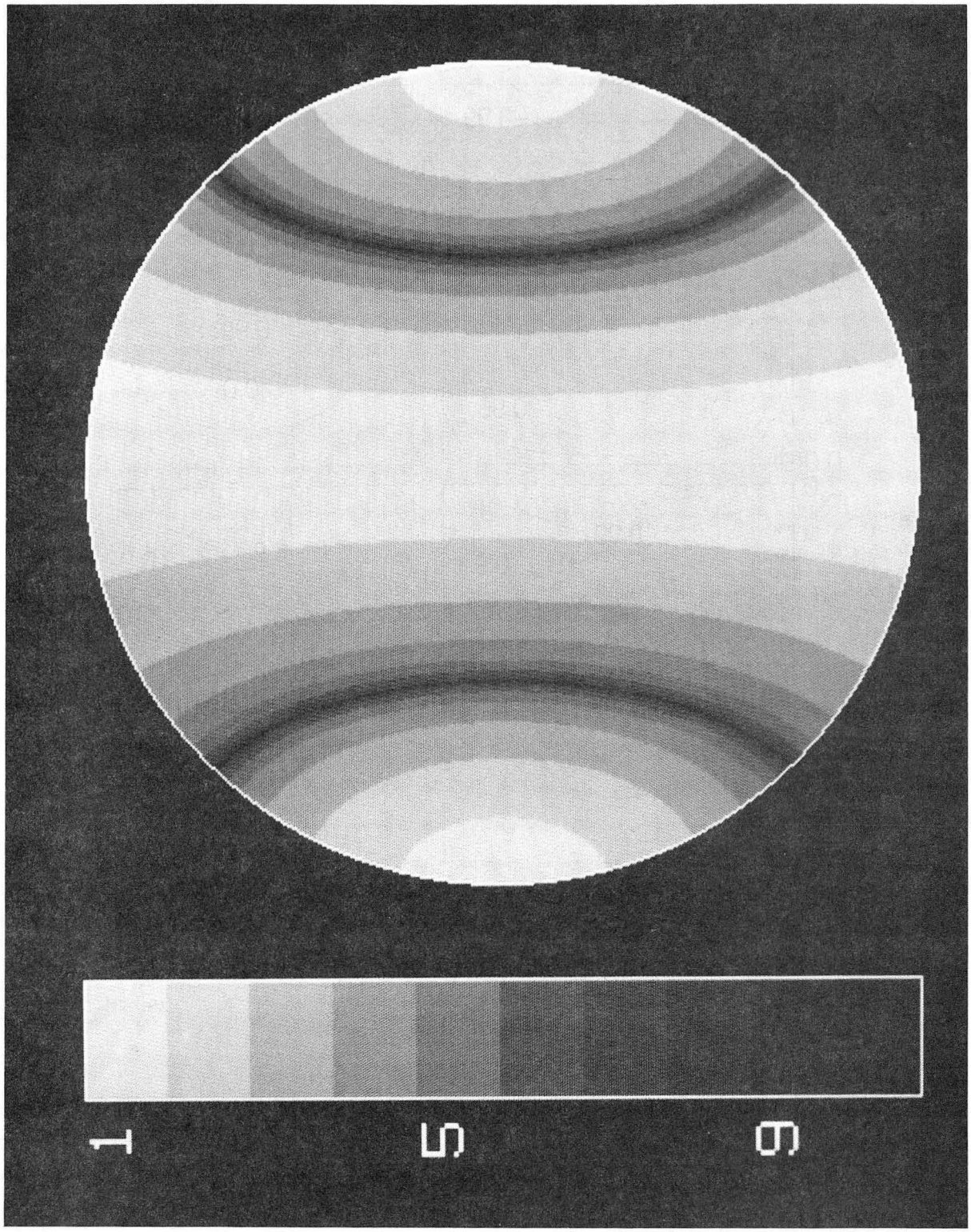

XBB 888-7861

Figure 6

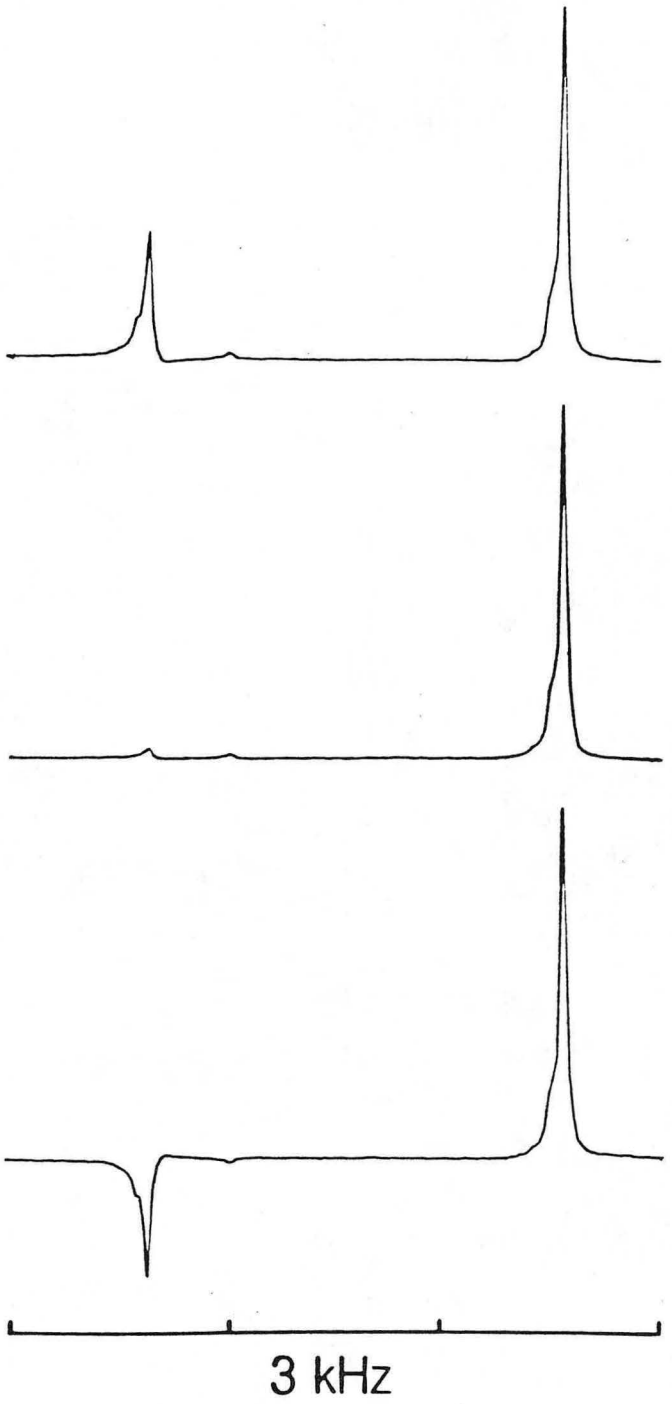

XBL 875-9286

Figure 7

LAWRENCE BERKELEY LABORATORY
TECHNICAL INFORMATION DEPARTMENT
UNIVERSITY OF CALIFORNIA
BERKELEY, CALIFORNIA 94720